HOKKAIDO UNIVERSITY

Title	Effectiveness of nano-scale ZSM-5 zeolite and its deactivation mechanism on catalytic cracking of representative hydrocarbons of naphtha
Author(s)	Konno, Hiroki; Tago, Teruoki; Nakasaka, Yuta et al.
Citation	Microporous And Mesoporous Materials, 175, 25-33 https://doi.org/10.1016/j.micromeso.2013.03.016
Issue Date	2013-07-15
Doc URL	https://hdl.handle.net/2115/53117
Type	journal article
File Information	Reviced Manuscript.pdf

Hokkaido University Collection of Scholarly and Academic Papers : HUSCAP

Title

Effectiveness of Nano-scale ZSM-5 Zeolite and its Deactivation Mechanism on Catalytic Cracking of Representative Hydrocarbons of Naphtha

Authors

Hiroki Konno, Teruoki Tago*, Yuta Nakasaka

Ryota Ohnaka, Jun-ichi Nishimura and Takao Masuda

Division of Chemical Process Engineering, Faculty of Engineering,

Hokkaido University, N13 W8, Kita-ku, Sapporo, Hokkaido 060-8628, Japan

** Corresponding author*

E-mail: tago@eng.hokudai.ac.jp

Tel:+81-117066551

Fax: +81-117066552

ZMPC 2012 paper

(Presentation No. P-158)

Abstract

The catalytic cracking of representative hydrocarbons of naphtha (*n*-hexane, cyclohexane, and methyl-cyclohexane) over ZSM-5 zeolite catalysts was examined at reaction temperatures ranging from 823 K to 923 K under atmospheric pressure. It was found that the Si/Al ratio of the zeolite affected the product selectivity and conversion. In order to investigate the effects of the crystal size of the ZSM-5 zeolites on catalyst lifetime, macro- and nano-scale ZSM-5 (Si/Al = 150) with crystal sizes of 2300 nm and 90 nm, respectively, were used for the cracking of representative naphtha hydrocarbons. In the cracking of naphthenes (cyclohexane and methyl-cyclohexane), coke was readily formed from the beginning of the reaction leading to significant deactivation of the catalyst for the macro-scale ZSM-5. In contrast, the nano-scale ZSM-5 exhibited a high conversion and high light olefins yield with stable activity, regardless of the type of reactant. As a result, the application of nano-scale ZSM-5 zeolites to the catalytic cracking of naphtha was effective and gave light olefins with high yield and excellent stable activity.

Keywords

catalytic cracking; naphtha; naphthenes; nano-zeolite; ZSM-5

1. Introduction

Light olefins, such as ethylene and propylene, are important basic raw materials for the petrochemical industry, and demand for light olefins is increasing every year [1, 2]. Light olefins have been mainly produced by thermal cracking of naphtha, which gives yields of ethylene and propylene of approximately 25% and 13%, respectively [3-5]. However, the capacity of the naphtha cracking process is not large enough to satisfy the increase in demand, because in this process, it is difficult to control the selectivity for specific light olefins. Moreover, because this process consumes more than 30% of the total amount of energy required in petrochemical refinement, developing efficient processes for the production of light olefins is indispensable. Unlike thermal cracking, catalytic cracking of naphtha over solid acid catalysts can be achieved at a high propylene/ethylene ratio at low reaction temperatures [6, 7], and thus using this process will reduce energy costs and provide selective production of propylene. Accordingly, the catalytic cracking of naphtha is expected to be an effective alternative to the thermal cracking process.

A promising catalyst for the catalytic cracking of naphtha is zeolite, a crystalline aluminosilicate material with various properties, such as strong acidity and a high surface area, and studies on the catalytic cracking of alkanes over zeolite catalysts have

been reported [8-16]. We have also studied the catalytic cracking of *n*-hexane over a ZSM-5 zeolite catalyst [17-19], in which it was revealed that ZSM-5 was effective for *n*-hexane cracking to light olefins synthesis. On the other hand, although naphthenes are important constituents of naphtha and affect the products generated from cracking [20], few studies have been published concerning the cracking of naphthenes [21-26] as compared to those of alkane cracking over zeolite catalysts. It is believed that not only alkane cracking, but also naphthene cracking, are indispensable in naphtha cracking, and thus both need to be investigated in order to gain a better understanding of naphtha cracking.

In the present study, the effect of the crystal size of a ZSM-5 (MFI-type) zeolite on the catalytic activity and light olefins yield in the catalytic cracking of representative hydrocarbons of naphtha was investigated. First, in order to optimize the reaction conditions for light olefins synthesis, the effects of reaction temperature and the Si/Al ratio of the ZSM-5 zeolite on *n*-hexane cracking were investigated. Next, the effect of the type of reactant on the catalyst lifetime and light olefins yield was examined using *n*-hexane, cyclohexane, and methyl-cyclohexane. Finally, the difference in the product selectivity and catalyst stability during alkane (*n*-hexane) and naphthene

(methyl-cyclohexane) cracking were investigated from the viewpoint of coke formation using nano- and macro-scale ZSM-5 zeolites.

2. Experimental

2.1 Preparation of ZSM-5 zeolites with different crystal sizes

The nano-scale ZSM-5 zeolite was prepared via hydrothermal synthesis using a water/surfactant/organic solvent (emulsion method [27-32]). An aqueous solution containing the Si and Al source materials was obtained by hydrolyzing each metal alkoxide in a dilute tetrapropyl ammonium hydroxide (TPAOH)/water solution. The water solution (10 ml) thus obtained was added to the surfactant/organic solvent (70 ml, surfactant concentration of 0.5 mol/l). Polyoxyethylene-(15)-oleylether and cyclohexane were employed as the surfactant and organic solvent, respectively. The water/surfactant/organic solvent thus obtained was poured into a Teflon-sealed stainless steel bottle and heated to 423 K for 72 h. In order to obtain the macro-scale ZSM-5, a hydrothermal synthesis was also carried out, but without the surfactant/organic solvent (conventional method). The molar compositions of the aqueous solution for the macro-scale ZSM-5 and the nano-scale ZSM-5 synthesis were SiO_2: $0.0033Al_2O_3$: 0.038NaOH: 0.10TPA: $355H_2O$ and SiO_2: $0.0017\text{-}0.01Al_2O_3$: 0.01-0.06NaOH:

0.33TPA: 33H_2O, respectively. The precipitates obtained from both methods were washed with alcohol, dried at 373 K for 12 h, and then calcined at 823 K for 3 h in an air stream. Physically adsorbed and/or ion-exchanged sodium ions on the zeolite surfaces were removed and exchanged with NH_4^+ using a conventional ion exchange technique with a 10% NH_4NO_3 aqueous solution, and then the zeolites were heated to 923 K to yield H-ZSM-5 zeolites. The powdered zeolites described above were pelletized, crushed, and sieved to yield samples ca. 0.3 mm in diameter for use in the catalytic cracking reactions.

2.2 Characterization

The morphology and crystallinity of the samples were analyzed using field emission scanning electron microscopy (FE-SEM; JSM-6500F, JEOL Co. Ltd.) and X-ray diffraction (XRD; JDX-8020, JEOL Co. Ltd.), respectively. The micropore volumes and the total and external surface areas of the samples were calculated using the BET- and the *t*-methods based on N_2 adsorption isotherms (Belsorp mini, BEL JAPAN Co. Ltd.). The Si/Al ratios of the samples were determined by X-ray fluorescence measurements (XRF; Supermini, Rigaku Co. Ltd.), and the acidity of the samples was evaluated via the ac-NH_3-TPD method [33] using TG. In the TPD

experiment, samples were first calcined under N_2 stream at 823 K, then cooled to 373 K. The gas was shifted from N_2 to 1.0 % NH_3 (balance He), and NH_3 molecules were adsorbed on the acid sites of the sample. After reaching adsorption/desorption equilibrium condition at 373K, a temperature of the reactor was increased from 373 K to 823 K at a heating rate of 5 K min^{-1}. The desorption of NH_3 molecules from the acid sites of the zeolite was measured under a 1.0% NH_3-He atmosphere so that the TPD profile could be measured under complete adsorption equilibrium conditions, which is referred to as the *ac*–NH_3–TPD method. In this method, the amount of NH_3 molecules desorbed from the sample above approximately 600 K were referred to the amount of strong acid sites on the sample.

2.3 Catalytic cracking of hydrocarbons over the ZSM-5 zeolites

Catalytic cracking of hydrocarbons over ZSM-5 zeolite catalysts was carried out using a fixed-bed reactor at reaction temperatures ranging from 823 K to 923 K under atmospheric pressure [17, 18]. The ZSM-5 zeolite catalyst was placed into a quartz tube reactor with inner diameter of 10 mm and calcined in flowing N_2 for 1 h at the reaction temperature before each run. In order to maintain the same volume of height in catalyst bed, the macro-scale ZSM-5 zeolite was mixed with quartz sand when

catalytic reaction. Meanwhile, the nano-scale ZSM-5 was not added anything when catalytic reaction. The *W/F* (*W*: amount of catalyst (g), *F*: feed rate (g h^{-1})) was 0.125 h or 0.15 h. In order to maintain a constant amount of carbon feed to the reactor, the partial pressure of hydrocarbons as feedstock was 22.1 kPa in the C6 feedstock (*n*-hexane and cyclohexane) and 18.9 kPa in the C7 feedstock (methyl-cyclohexane) at the inlet of the reactor. The feed rate of the hydrocarbons as feedstock was 8.22×10^{-2} C-mol/h. The composition of the exit gas was measured using an on-line gas chromatograph (GC-2014, Shimadzu Co. Ltd.) with a Porapak-Q column for the thermal conductivity detector (TCD) and Gaskuropack-54 and SP-1700 columns for the flame ionization detectors (FIDs). The amount of coke deposited on the catalyst after the reaction was measured via thermogravimetric analysis (TG; TGA-50, Shimadzu Co. Ltd.). Although aromatics with high vaporization temperature such as benzene, toluene and xylene are formed during the reaction, all products were measured using on-line gas chromatograph through the pre-heater at 410 K. Total carbon yields of these products were approximately 90-98 C-mol% in each cracking reactions.

3. Results and discussion

3.1 Characterization of synthesized ZSM-5 zeolites with different crystal sizes

To investigate the effect of the Si/Al ratio of the ZSM-5 zeolites on the product selectivity and yield, nano-scale ZSM-5 with different Si/Al molar ratios (50, 150, and 300) were prepared via hydrothermal synthesis in a water/surfactant/organic solvent [27]. Figs. 1 and 2 show the X-ray diffraction patterns and FE-SEM micrographs of the samples, respectively. The X-ray diffraction patterns of the samples with different Si/Al ratios showed peaks corresponding to an MFI-type zeolite. Moreover, nano-scale zeolites with crystal sizes of approximately 90 nm were observed. The XRD pattern and FE-SEM micrograph of a macro-scale zeolite are also shown for comparison and to illustrate the macro-scale zeolite (Si/Al = 150) with a crystal size of approximately 2300 nm. As can be seen in Table 1, while the external surface area increased with decreasing crystal size, the micropore volume (0.18 cm^3/g) and the BET surface area (400 m^2/g) were nearly constant, regardless of the crystal size. Fig. 3 and Table 1 show the NH_3-TPD profiles and Si/Al ratios as determined by XRF analysis of the zeolites with different crystal sizes and Si/Al ratios, respectively. The Si/Al values were nearly the same for each Si/Al ratio, which was calculated from the Si and Al concentrations in the corresponding synthetic solution, indicating that the Al atoms in the synthetic solutions were incorporated into the framework structures of the ZSM-5 zeolites during the hydrothermal synthesis. NH_3 desorption peaks at temperatures above 600 K that are

associated with strong acid sites were also observed. In addition, the area of the TPD profiles above 600 K depended on the Si/Al ratio of the zeolites. Therefore, ZSM-5 zeolites with different crystal sizes and acid densities were obtained, and these various zeolites were used as catalysts for the cracking reaction.

3.2 Product distribution and light olefins yields for n-hexane cracking over ZSM-5 zeolites with different Si/Al ratios

First, the effects of reaction temperature and Si/Al ratio on the catalytic activity and product selectivity of *n*-hexane cracking were examined using the nano-scale ZSM-5 catalysts. Fig. 4 shows the results of *n*-hexane cracking over nano-scale ZSM-5 catalysts with different Si/Al ratios at reaction temperatures ranging from 823 K to 923 K. In the case of thermal cracking without the catalyst, the *n*-hexane conversion was 1.2 %, 4.8 %, and 20.0 % at 823 K, 873 K, and 923 K, respectively. As can be seen in Fig. 4, the conversion of n-hexane depended on both the Si/Al ratio and the reaction temperature. The dependency of *n*-hexane conversion indicated that the reaction progressed over the acid sites of the zeolite. The product selectivities are listed in Table 2 in detail. Products including alkanes (methane, ethane, propane, and butanes), alkenes (ethylene, propylene, and butenes), and aromatics (benzene, toluene, and xylene (BTX))

were obtained. It should be noted, however, that, because a detailed analysis was difficult, the amounts of C_5 and C_7^+ alkanes and alkenes listed in Table 2 are collectively denoted as paraffins in Fig. 4.

As the reaction temperature increased, the light olefins and BTX selectivities increased (e.g., the total selectivity of unsaturated hydrocarbons, such as ethylene, propylene, butenes, and BTX, was 52.1 %, 60.4 %, and 67.3 % at reaction temperatures of 823 K, 873 K, and 923 K, respectively, in the case of Si/Al = 150) and the paraffin selectivity decreased for each of the ZSM-5 zeolites (e.g., the total selectivity of saturated hydrocarbons, such as ethane, propane, and butanes was 43.3 %, 35.0 %, and 26.0 % at reaction temperatures of 823 K, 873 K, and 923 K, respectively, in the case of Si/Al = 150). This change in selectivity occurs because dehydrogenation (e.g., paraffin to olefin), proceeds readily at high temperature [34]. As can be seen in Fig. 4, ZSM-5 (Si/Al = 150) exhibited the highest light olefins yield (50.4 %) at 923 K, because excessive reactions, such as the consumption of light olefins and BTX formation, were suppressed by the low acid density (i.e., high Si/Al ratio). Accordingly, the application of ZSM-5 zeolite (Si/Al = 150) to the cracking reaction at a high reaction temperature of 923 K was effective for improving the light olefins yield. Thus, in order to investigate the effect of the crystal size of the ZSM-5 zeolites on the catalytic activity, these

optimized reaction conditions (Si/Al = 150, T = 923 K) were used for the extended cracking reaction of *n*-hexane, cyclohexane, and methyl-cyclohexane.

3.3 Catalytic stability of ZSM-5 zeolites with different crystal sizes on the n-hexane, cyclohexane and methyl-cyclohexane cracking

The effect of the zeolite crystal size on the stability of the catalyst activity during catalytic cracking of representative naphtha hydrocarbons, such as *n*-hexane, cyclohexane, and methyl-cyclohexane, was investigated using ZSM-5 zeolites (Si/Al = 150) with different crystal sizes (90 nm and 2300 nm). Although the molecular size of cyclohexane (approximately 0.6nm) is slightly larger than the pore size of ZSM-5 zeolite, the cyclohexane molecules can diffuse into the pore of MFI-type zeolite due to thermal vibration and expansion of the pore opening [35, 36]. Moreover, because the minimum molecular size of methyl-cyclohexane is as same as the size of cyclohexane, it is considered that the methyl-cyclohexane also can diffuse into the pore of MFI-type zeolite. The conversions, product selectivities and olefin yields are shown in Figs. 5-7. The micropore volumes of the ZSM-5 zeolites and the amount of coke generated after the cracking reaction were measured (Table 3). In the thermal cracking without the catalyst, the *n*-hexane, cyclohexane, and methyl-cyclohexane conversions were 20.0 %,

1.0 %, and 5.6 %, respectively, under these reaction conditions.

As can be seen in Fig. 5, because the nano- and macro-scale zeolites exhibited nearly the same acidity as shown in Fig. 3, the initial conversion of *n*-hexane cracking was nearly the same (approximately 83 %). While the conversion slightly decreased with time on-stream in the macro-scale ZSM-5, the nano-scale ZSM-5 maintained a high conversion, barely changing from the beginning of the reaction. In the macro-scale zeolite, the diffusion resistance of the produced light olefins within the crystal induced further reactions, resulting in the production of aromatics and coke. Accordingly, a slightly high BTX selectivity and a large amount of coke deposition were observed with the macro-scale zeolite as compared to that obtained with the nano-scale zeolite. In contrast, the stable activity of the nano-scale ZSM-5 yielded stable product selectivities as compared to those obtained for the macro-scale ZSM-5. It is considered that the decrease in the crystal size caused a decrease in the diffusion resistance (D/L^2, D: diffusivity [m^2/s], L: crystal size [m]) and an increase in the external surface area (Table 1). The small diffusion resistance was expected to suppress the excessive reaction of the produced light olefins. Moreover, the large external surface area led to the large number of pore mouths, which should retard the deactivation resulting from pore plugging by coke formed during the reaction.

In Figs. 6 and 7, the effect of the crystal size of the zeolite on the stability of naphthene (cyclohexane and methyl-cyclohexane) conversion is clearly observed. Moreover, the changes in the conversion and product selectivity of naphthene cracking were very different from those observed for *n*-hexane cracking. Although the nano-scale zeolite maintained a high conversion for naphthene cracking (Figs. 6(b) and 7(b)), the conversion of cyclohexane and methyl-cyclohexane decreased considerably with reaction time with the macro-scale zeolite (Figs. 6(a) and 7(a), respectively). The considerable deactivation of the macro-scale zeolite was ascribed to the large diffusion resistance of naphtenes and production of BTX. Because not only the cracking reaction, but also dehydrogenation reactions, such as "cyclohexane to benzene" and "methyl-cyclohexane to toluene", readily occurred [25, 26], the selectivity for which was higher in naphthene cracking than in *n*-hexane cracking.

BTX (i.e., a coke precursor) was one of the primary products of naphthene cracking, followed by coke formation. On the other hand, in *n*-hexane cracking, the BTX was the terminating product derived from a sequential reaction of the produced light olefins, and not the primary product [17, 18]. For these reasons, the deactivation rate in the cracking of the naphthenes was faster than that in the cracking of *n*-hexane. Additionally, because coke was easily formed during the initial stages of the reaction

near the external surface of the macro-scale ZSM-5 due to the large diffusion resistance of naphthenes, the macro-scale ZSM-5 was seriously deactivated. Probably, in the methyl-cyclohexane cracking over ZSM-5 zeolites at initial reaction time (*i.e.* 0 minute), macro-scale ZSM-5 shows similar finding to nano-scale ZSM-5 about the methyl-cyclohexane conversion. However, because the macro-scale ZSM-5 was rapidly deactivated in the methyl-cyclohexane cracking, the conversion after 20 minutes was already decreased. By contrast, the nano-scale ZSM-5 exhibited a high light olefins yield and excellent stability (Figs. 6 and 7) for propylene. Accordingly, the application of the nano-scale ZSM-5 was effective for naphtha cracking, leading to a stable propylene/ethylene carbon-molar ratio (P/E ratio) of approximately 2.0, regardless of the reactants used. Moreover, the P/E ratios in the cracking reactions using the nano-scale ZSM-5 were much higher than the values for thermal cracking (0.5-0.6 [37]).

3.4 Deactivation of the nano-scale ZSM-5 catalyst during cracking reactions

As compared with the macro-scale ZSM-5, the nano-scale ZSM-5 exhibited stable activity and high light olefin yields with *n*-hexane, cyclohexane, and methyl-cyclohexane. However, a slight decrease in the catalytic activity was observed

in the cracking reactions of cyclohexane and methyl-cyclohexane (Figs. 6(b) and 7(b), respectively), possibly due to BTX production followed by coke formation. In addition, in Table 3, whereas the micropore volume of the nano-scale ZSM-5 zeolite was nearly unchanged after *n*-hexane cracking, the volumes were clearly decreased after naphthene cracking for 4.5 h. These results suggest that the difference in the deactivation mechanism for n-hexane and naphthene cracking is ascribed to a decrease in the micropore volume due to coke formation. Next, in order to confirm the reason for the difference in the deactivation mechanism of n-hexane and naphthene cracking, the cracking of *n*-hexane and methyl-cyclohexane was carried out using the nano-scale ZSM-5 for 4.5 h, 10 h, and 15 h. Fig. 8 shows the changes in the *n*-hexane and methyl-cyclohexane conversions with time on-stream. The N_2 adsorption isotherms and the NH_3-TPD profiles of the nano-scale ZSM-5 zeolites after the cracking reactions for each reaction time (4.5 h, 10 h, and 15 h) are shown in Figs. 9 and 10, respectively. The amount of coke on the nano-scale ZSM-5 zeolites and their micropore volumes after cracking are also listed in Table 3.

In the cracking of *n*-hexane, although the amount of coke increased to 13.7 wt % after 15 h, the nitrogen adsorption isotherm and micropore volume of the zeolite was nearly unchanged, and the acidity of the zeolite was only slightly decreased with

reaction time. These results suggest that the coke was mainly deposited on the external surface of the zeolite crystal, and that acid sites without coke remained inside the crystal, leading to the slight decrease in the catalytic activity observed in Fig. 8. Moreover, the large external surface area of the nano-scale zeolite supported the longer catalyst lifetime as compared with that of the macro-scale zeolite.

In contrast, in the cracking of methyl-cyclohexane, as the amount of coke increased, the micropore volume and the acidity of the zeolite gradually decreased. These results indicate that significant pore plugging and/or coke formation occurred on the acid sites. As mentioned above, in addition to formation of light olefins via the cracking reaction, aromatics were also produced as primary products via dehydrogenation on the pore surface inside the crystal [25, 26], which were then adsorbed onto the acid sites, followed by formation of heavy hydrocarbons and pore plugging. Accordingly, these results suggest that coke formation occurred on the external surface as well as inside the crystal, leading to the gradual decrease in the catalytic activity observed in Fig. 8.

As discussed above, the coke derived from *n*-hexane cracking was mainly deposited on the external surface of the zeolite crystal, and that derived from methyl-cyclohexane cracking was deposited on the external surface as well as inside the

crystal. In naphthenes cracking, the coke deposited within the crystal induced the serious deactivation of the zeolite catalyst due to the decrease in micropore volume and acidity. However, the nano-scale zeolite could maintain a longer catalyst lifetime regardless of type of reactant due to the large external surface area and low diffusion resistance to the reactant/product hydrocarbons compared to that of the macro-scale zeolite.

Conclusion

The catalytic cracking of representative hydrocarbons of naphtha over ZSM-5 zeolite catalysts was examined at reaction temperatures ranging from 823 K to 923 K under atmospheric pressure. It was found that the Si/Al ratio of the ZSM-5 affected the product selectivity and conversion, and that application of ZSM-5 (Si/Al = 150) was effective in improving the light olefins yield for *n*-hexane cracking. In addition, the effect of crystal size on catalytic stability in the catalytic cracking of representative naphtha hydrocarbons was investigated using ZSM-5 zeolites. The deactivation mechanism and catalyst lifetime of the zeolite catalyst depended on the type of reactant, and the deactivation of the zeolite in the cracking of naphthenes was greater than that in the cracking of *n*-hexane. However, compared to the macro-scale ZSM-5, the

nano-scale ZSM-5 exhibited a high conversion and high light olefins yield with stable activity, regardless of the type of reactant. As a result, the application of the nano-scale ZSM-5 zeolite was effective for the catalytic cracking of naphtha.

5

References

[1] O. Bortnovsky, P. Sazama, B. Wichterlova, *Appl. Catal. A*, **287** (2005) 203

[2] C. Mei, P. Wen, Z. Liu, Y. Wang, W. Yang, Z. Xie, W. Hua, Z. Gao, *J. Catal.*, **258** (2008) 243

[3] J.S. Jung, J.W. Park, G. Seo, *Appl. Catal. A*, **288** (2005) 149

[4] T. Komatsu, H. Ishihara, Y. Fukui, T. Yashima, *Appl. Catal. A*, **214** (2001) 103

[5] J.S. Plotkin, *Catal. Today*, **106** (2005) 10

[6] Y. Yoshimura, N. Kijima, T. Hayakawa, K. Murata, K. Suzuki, F. Mizukami, K. Matano, T. Konishi, T. Oikawa, M. Saito, T. Shiojima, K. Shiozawa, K. Wakui, G. Sawada, K. Sato, S. Matsuo, N. Yamaoka, *Catal. Surv. Jpn.*, **4** (2000) 157

[7] A. Corma , A.V. Orchillès, *Micropor. Mesopor. Mater.*, **35** (2000) 21

[8] N. Katada, Y. Kageyama, K. Takahara, T. Kanai, H.A. Beguma, M. Niwa, *Catal., A Chem.* **211** (2004) 119

[9] H. Mochizuki, T. Yokoi, H. Imai, R. Watanabe, S. Namba, J. N. Kondo, T. Tatsumi, *Micropor. Mesopor. Mater.*, **145** (2011)165

[10] K. Kubo, H. Iida, S. Namba, A. Igarashi, *Micropor. Mesopor. Mater.*, **149** (2012)126

[11] S. Inagaki, K. Takechi, Y. Kubota, *Chem. Comm.*, **46** (2010) 2662

[12] S.M.T. Sendesi, J. Towfighi, K. Keyvanloo, *Catal. Comm*., 27 (2012) 114

[13] A. Corma, J. Mengual, P.J. Miguel, *Appl. Catal. A*, **421-422** (2012) 121

[14] A. Corma, J. Mengual, P.J. Miguel, *Appl. Catal. A*, **417-418** (2012) 220

[15] G. Liu, G. Zhao, F. Meng, S.Qu, L. Wang, X. Zhang, *Energ Fuel*, **26** (2012) 1220

[16] S. Qu, G. Liu, F. Meng, L. Wang, X. Zhang, *Energ Fuel*, **25** (2011) 2808

[17] H. Konno, T. Okamura, Y. Nakasaka, T. Tago, T. Masuda, *J. Jpn. Petrol. Inst.*, **55** (2012) 267

[18] H. Konno, T. Okamura, Y. Nakasaka, T. Tago, T. Masuda, *Chem. Eng. J.*, **207-208** (2012) 490

[19] T. Tago, H. Konno, Y. Nakasaka, T. Masuda, *Catal. Surv. Asia*, **16** (2012) 148

[20] P.B. Venuto and E.T. Habib, *Catal. Rev. Sci. Eng.*, **18** (1978) 1.

[21] A. Corma, A. Agudo, *Catal. Lett.*, **16** (1981) 253.

[22] A. Corma, F. Mocholi, V. Orchillès, *Appl. Catal. A*, **67** (1990) 307

[23] J. Abbot, B. Wojciechowski, *J. Catal.*, **107** (1987) 571.

[24] J. Abbot, *J. Catal.*, **123** (1990) 383

[25] H.S. Cerqueira, P.C. Mihindou-Koumba, P. Magnoux, M. Guisnet, *Ind. Eng. Chem. Res.*, **40** (2001) 1032

[26] A. Slagtern, I.M. Dahl, K.J. Jens, T. Myrstad, *Appl. Catal. A*, **375** (2010) 213

[27] T. Tago, M. Nishi, Y. Kouno, T. Masuda, *Chem. Lett.*, **33** (2004) 1040

[28] T. Tago, K. Iwakai, M. Nishi, T. Masuda, *J. Nanosci. Nanotechnol.*, **9** (2009) 612

[29] T. Tago, D. Aoki, K. Iwakai, T. Masuda, *Top. Catal*., **52** (2009) 865

[30] T. Tago, M. Sakamoto, K. Iwakai, H. Nishihara, S.R. Mukai, T. Tanaka, T. Masuda, *J. Chem. Eng. Jpn*., **42** (2009) 162

[31] K. Iwakai, T. Tago, H. Konno, Y. Nakasaka, T. Masuda, *Micropor. Mesopor. Mater.*, **141** (2011) 167

[32] T. Tago, Y. Nakasaka, T. Masuda, *J. Jpn. Petrol. Inst.*, **55** (2012) 149

[33] T. Masuda, Y. Fujikata, S. R. Mukai, K. Hashimoto, *Appl. Catal. A Gen.*, **165** (1997) 57

[34] M.M. Bhasin, J.H. McCain, B.V. Vora, T. Imai, P.R. Pujado, *Appl. Catal. A*, **221** (2001) 397

[35] L. Song, L.V.C. Rees, *Micropor. Mesopor. Mater.*, **35-36** (2000) 301

[36] L. Song, Z. Sun, L. Duan, J. Gui, G.S. McDougall, *Micropor. Mesopor. Mater.*, **104** (2007) 115

[37] S.M. Sadrameli, A.E.S. Green, *J. Anal. Appl. Pyrol.*, **73** (2005) 305

Figure and Table Captions

Fig. 1. XRD patterns of ZSM-5 zeolites with different Si/Al ratios and crystal sizes.

Fig. 2. SEM micrographs of ZSM-5 zeolites with different Si/Al ratios and crystal sizes.

Fig. 3. NH_3-TPD profiles of ZSM-5 zeolites with different Si/Al ratios and crystal sizes.

Fig. 4. Product selectivities and light olefin yields for the *n*-hexane cracking reaction (*W/F* = 0.15 h) over nano-scale ZSM-5 zeolites with different Si/Al ratios at reaction temperatures ranging from 823 K to 923 K.

Fig. 5. Conversions, product selectivities, and light olefin yields for *n*-hexane cracking (*W/F* = 0.125 h) over (a) macro-scale ZSM-5 and (b) nano-scale ZSM-5 (Si/Al = 150).

Fig. 6. Conversions, product selectivities, and light olefin yields for cyclohexane cracking (*W/F* = 0.125 h) over (a) macro-scale ZSM-5 and (b) nano-scale ZSM-5 (Si/Al = 150).

Fig. 7. Conversions, product selectivities, and light olefin yields for methyl-cyclohexane cracking (*W/F* = 0.125 h) over (a) macro-scale ZSM-5 and (b) nano-scale ZSM-5 (Si/Al = 150).

Fig. 8. (a) *n*-Hexane and (b) methyl-cyclohexane conversions with time on-stream (*W/F* = 0.125 h) over the nano-scale ZSM-5 zeolite (Si/Al = 150).

Fig. 9. N_2 adsorption isotherms of ZSM-5 zeolites before and after (a) *n*-hexane and (b) methyl-cyclohexane cracking reactions (4.5 h, 10 h, and 15 h).

Fig. 10. NH_3-TPD profiles of nano-scale ZSM-5 zeolites (Si/Al = 150) before and after (a) *n*-hexane and (b) methyl-cyclohexane cracking reactions.

Table 1. Micropore volumes, BET surface areas, external surface areas, and Si/Al ratios of ZSM-5 zeolites. V_m: micropore volume using the *t*-method, S_{BET}: surface area using the BET method, S_{ext}: external surface area using the *t*-method.

Table 2. Product selectivities for *n*-hexane cracking (*W/F* = 0.15 h) over nano-scale ZSM-5 zeolites with different Si/Al ratios.

Table 3. Coke amounts and micropore volumes of ZSM-5 zeolites (Si/Al = 150) after cracking of *n*-hexane, cyclohexane and methyl-cyclohexane (*W/F* = 0.125 h) determined using TG and the *t*-method.

Zeolite (Si/Al)	V_m (cm^3g^{-1})	S_{BET} (m^2g^{-1})	S_{ext} (m^2g^{-1})	Si/Al measured by XRF
nano-scale ZSM-5 (50)	0.17	389	42.0	58
nano-scale ZSM-5 (150)	0.18	395	35.3	183
nano-scale ZSM-5 (300)	0.18	397	36.0	389
macro-scale ZSM-5 (150)	0.18	402	5.9	154

Table 1. Micropore volumes, BET surface areas, external surface areas, and Si/Al ratios of ZSM-5 zeolites. V_m: micropore volume using the *t*-method, S_{BET}: surface area using the BET method, S_{ext}: external surface area using the *t*-method.

Temperature	Si/Al	Conversion [C-mol%]	Product selectivity [C-mol%]									
			CH_4	C_2H_4	C_2H_6	C_3H_6	C_3H_8	C_4H_8	C_4H_{10}	C_5	C_7^+	BTX
823K	50	72.3	2.4	14.2	9.2	23.6	21.3	4.0	10.2	2.8	0.1	12.1
	150	58.5	1.7	14.5	9.6	28.7	22.2	4.8	11.5	3.0	0.1	4.1
	300	17.5	2.2	7.2	11.6	32.1	15.1	9.3	17.7	4.1	0.0	0.7
	without catalyst	1.2	9.1	19.4	8.3	21.5	0.8	0.0	17.1	23.8	0.0	0.0
873K	50	93.1	4.5	17.4	8.7	21.2	14.2	2.8	6.9	1.9	0.0	22.3
	150	81.8	3.1	17.6	10.1	29.5	15.5	4.1	9.4	1.9	0.0	9.2
	300	38.2	2.7	10.2	11.2	35.0	13.4	7.9	15.4	2.6	0.0	1.6
	without catalyst	4.8	10.4	24.7	8.5	24.8	0.6	0.2	18.7	12.1	0.0	0.0
923K	50	99.4	7.0	22.0	8.1	17.9	9.5	1.6	3.5	0.8	0.0	29.7
	150	95.7	5.5	22.1	9.1	27.6	10.6	2.9	6.3	1.1	0.0	14.7
	300	66.7	3.9	16.3	10.5	36.2	10.4	6.1	11.9	1.8	0.2	2.8
	without catalyst	20.0	11.1	30.0	7.6	25.9	0.4	0.3	17.1	7.7	0.0	0.0

Table 2. Product selectivities for *n*-hexane cracking (*W/F* = 0.15 h) over nano-scale ZSM-5 zeolites with different Si/Al ratios.

Reactant	Catalyst	Reaction time [h]	Coke amount [wt%]	V_m [cm^3g^{-1}]
-	macro-scale ZSM-5	0	0	0.18
	nano-scale ZSM-5	0	0	0.18
n-hexane	macro-scale ZSM-5	4.5	7.1	0.15
	nano-scale ZSM-5	4.5	1.5	0.18
		10.0	4.4	0.17
		15.0	13.7	0.17
cyclohexane	macro-scale ZSM-5	4.5	7.4	0.11
	nano-scale ZSM-5	4.5	2.8	0.17
methyl-cyclohexane	macro-scale ZSM-5	4.5	6.9	0.10
	nano-scale ZSM-5	4.5	5.1	0.16
		10.0	10.0	0.15
		15.0	13.3	0.14

Table 3. Coke amounts and micropore volumes of ZSM-5 zeolites (Si/Al = 150) after cracking of *n*-hexane, cyclohexane and methyl-cyclohexane (*W/F* = 0.125 h) determined using TG and the *t*-method.

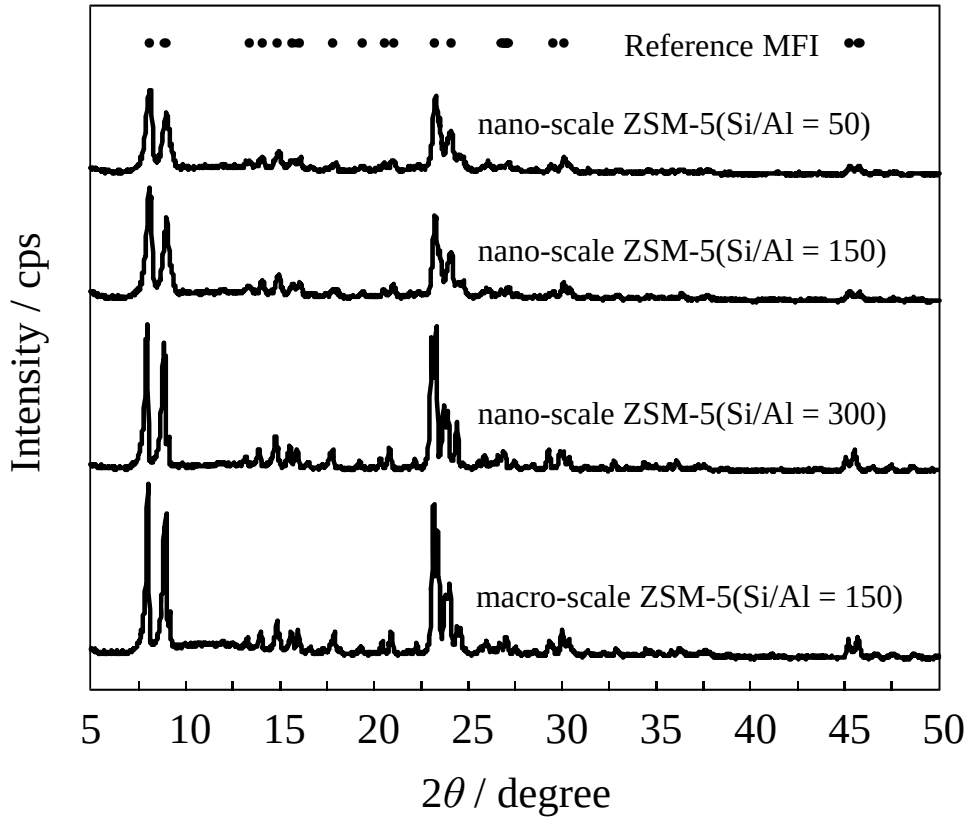

Fig. 1. XRD patterns of ZSM-5 zeolites with different Si/Al ratios and crystal sizes.

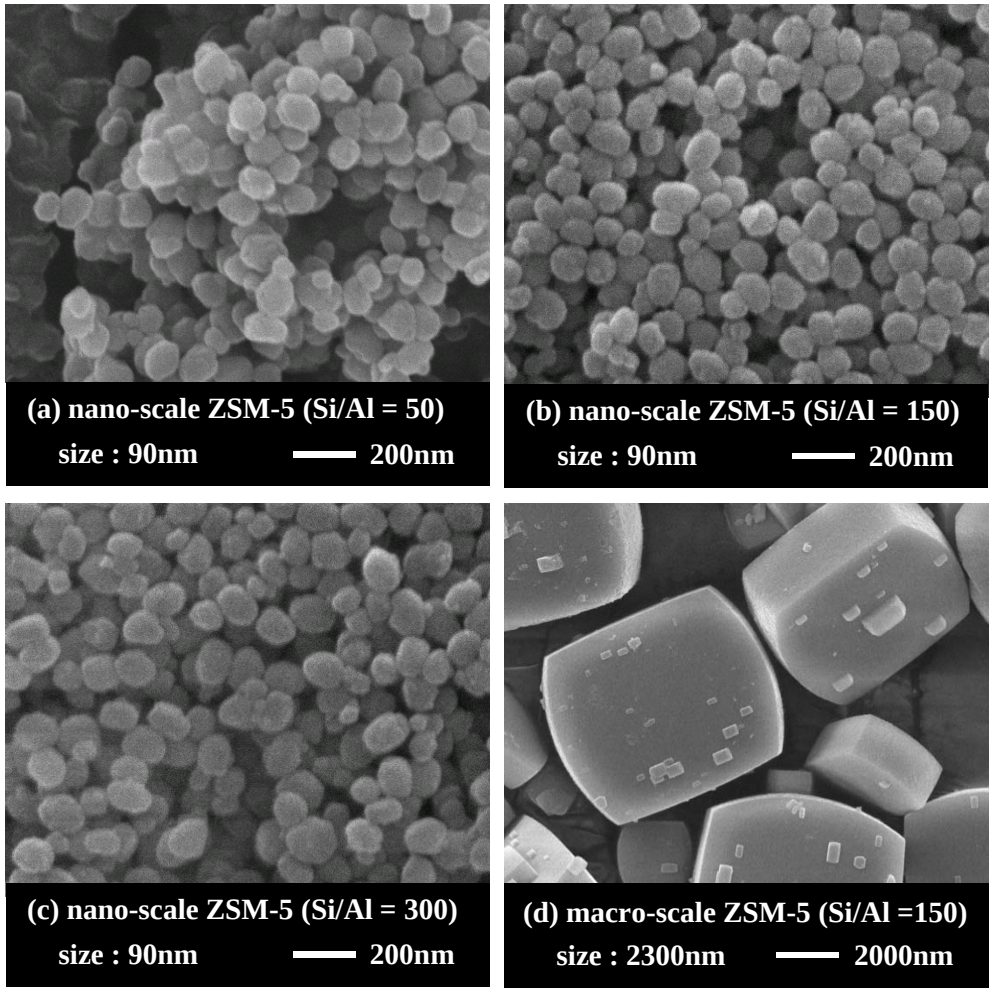

Fig. 2. SEM micrographs of ZSM-5 zeolites with different Si/Al ratios and crystal sizes.

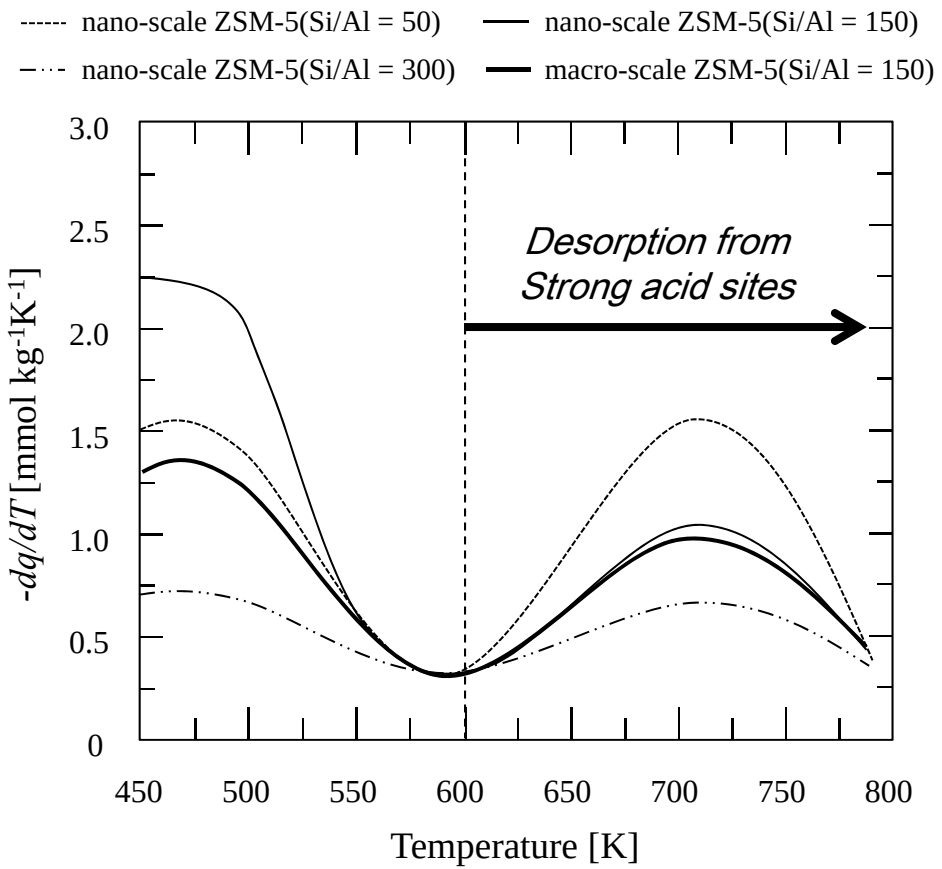

Fig. 3. NH_3-TPD profiles of ZSM-5 zeolites with different Si/Al ratios and crystal sizes.

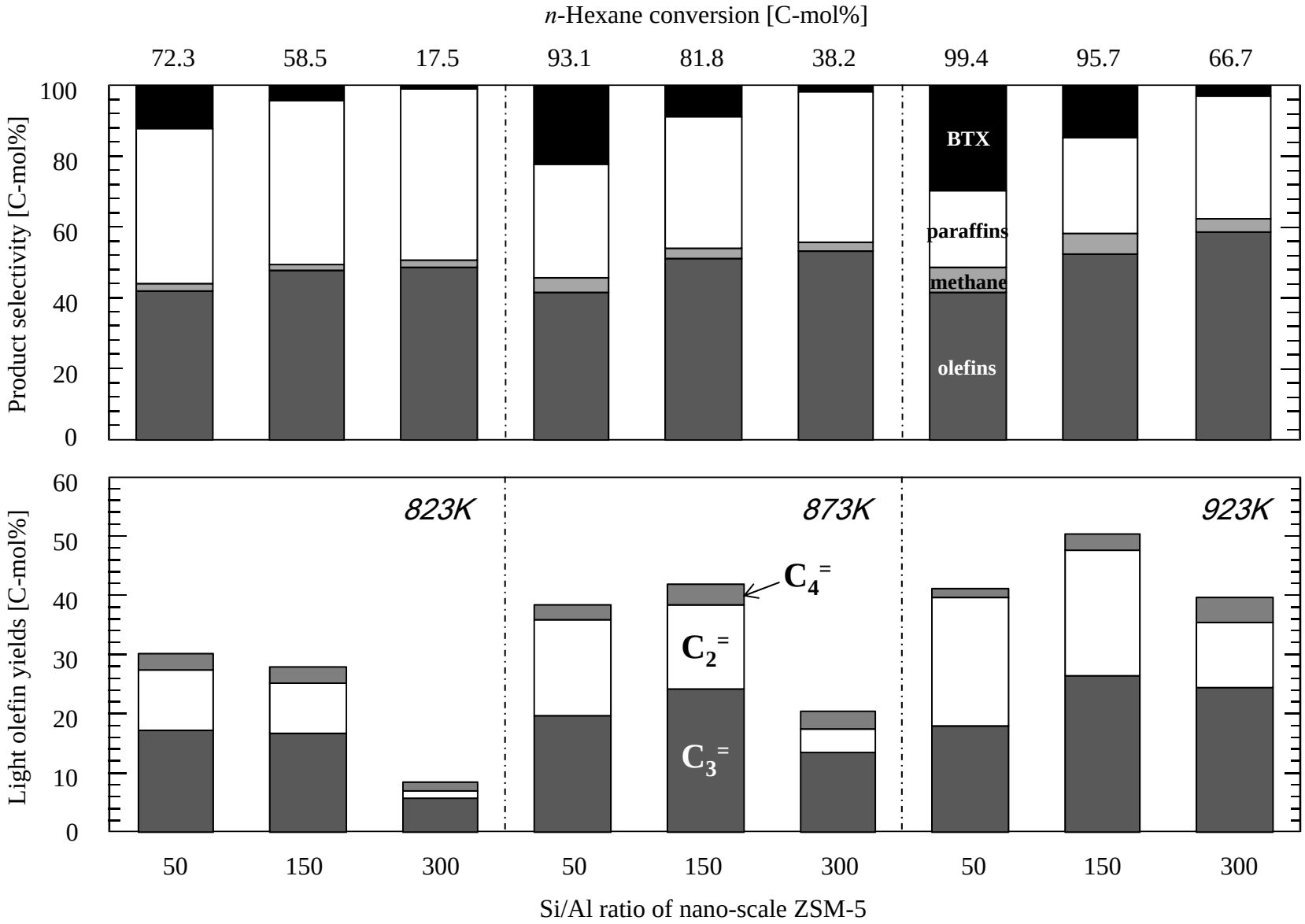

Fig. 4. Product selectivities and light olefin yields for the *n*-hexane cracking reaction (*W/F* = 0.15 h) over nano-scale ZSM-5 zeolites with different Si/Al ratios at reaction temperatures ranging from 823 K to 923 K.

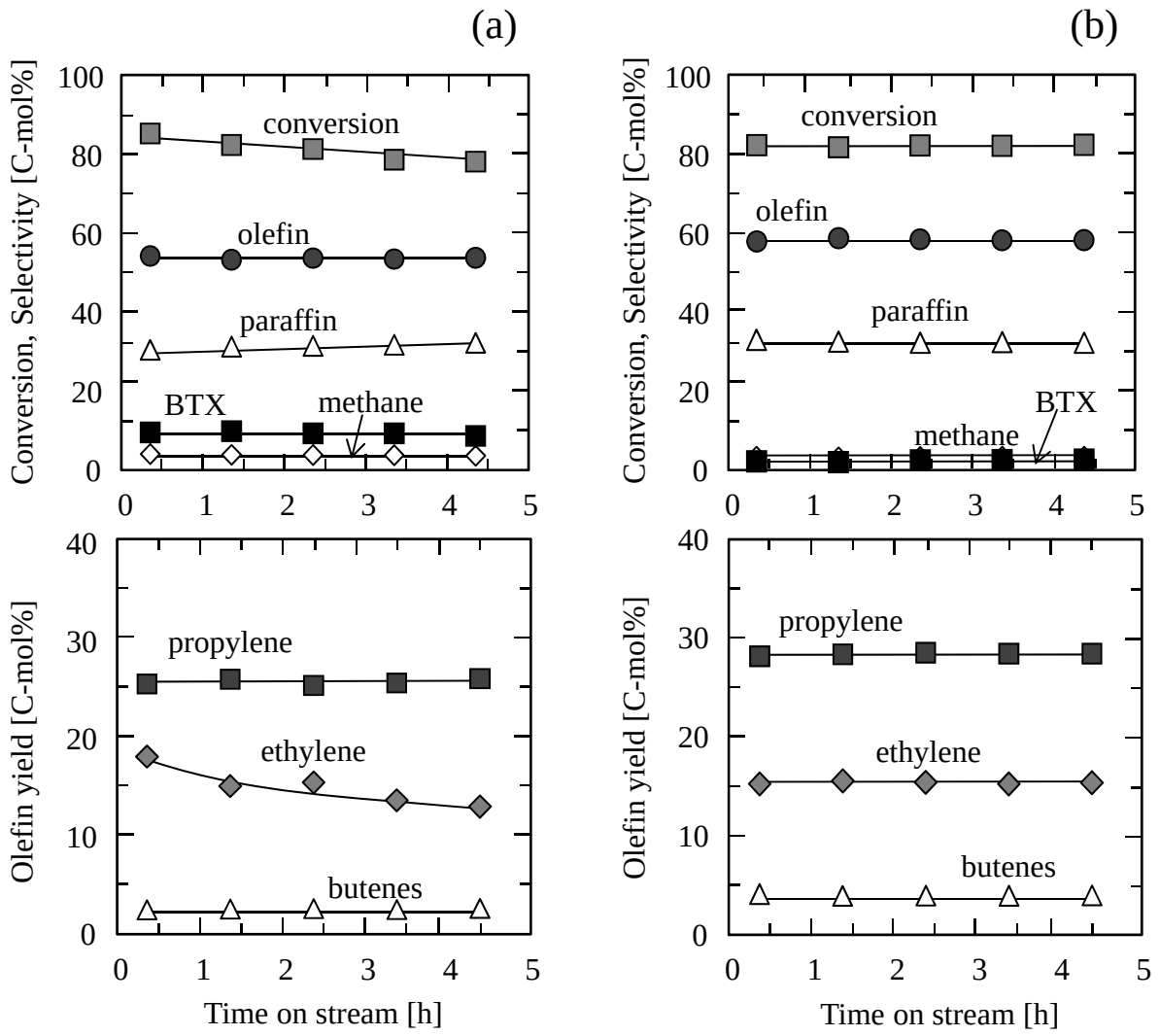

Fig. 5. Conversions, product selectivities, and light olefin yields for *n*-hexane cracking (*W/F* = 0.125 h) over (a) macro-scale ZSM-5 and (b) nano-scale ZSM-5 (Si/Al = 150).

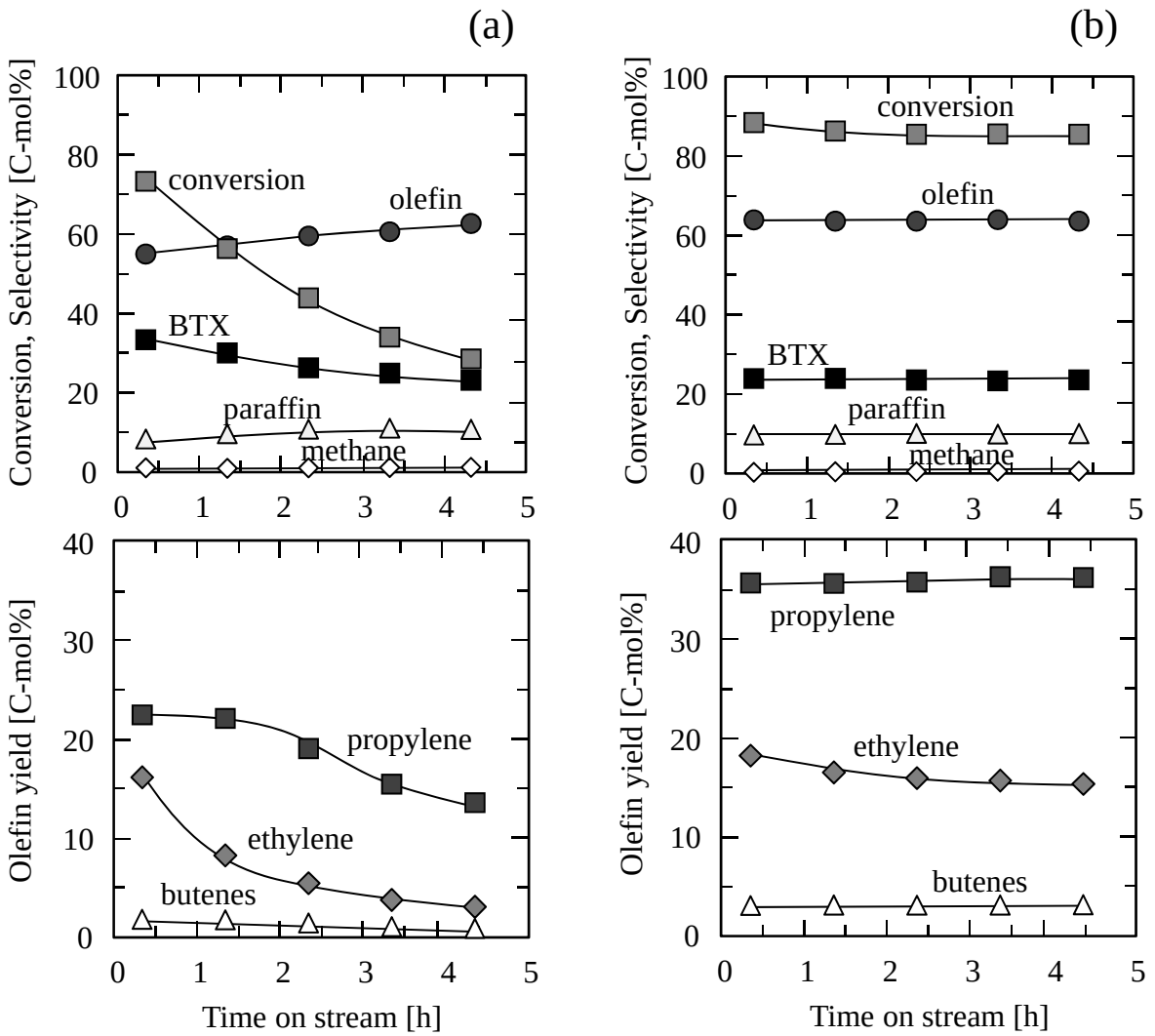

Fig. 6. Conversions, product selectivities, and light olefin yields for cyclohexane cracking (*W/F* = 0.125 h) over (a) macro-scale ZSM-5 and (b) nano-scale ZSM-5 (Si/Al = 150).

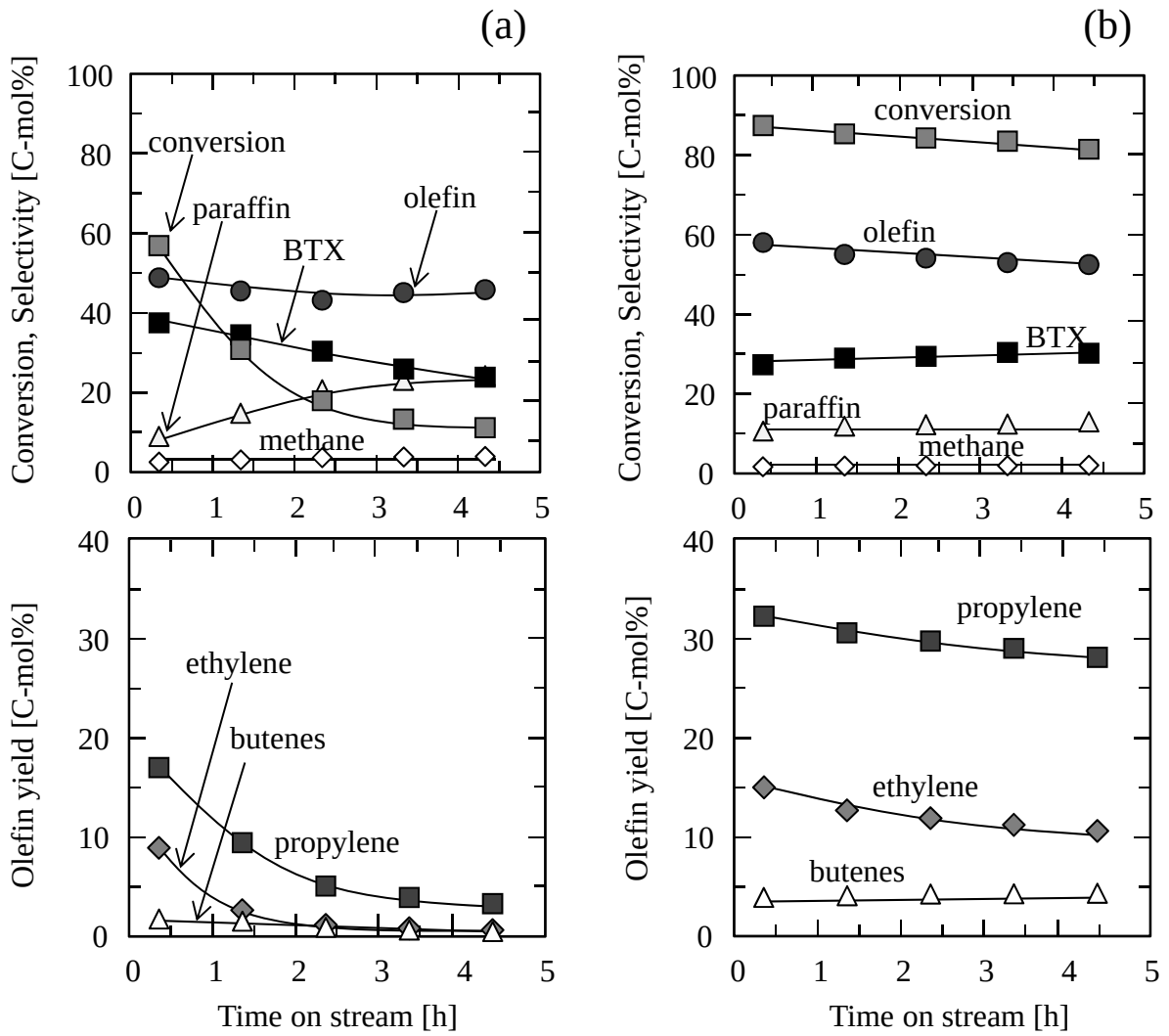

Fig. 7. Conversions, product selectivities, and light olefin yields for methyl-cyclohexane cracking (*W/F* = 0.125 h) over (a) macro-scale ZSM-5 and (b) nano-scale ZSM-5 (Si/Al = 150).

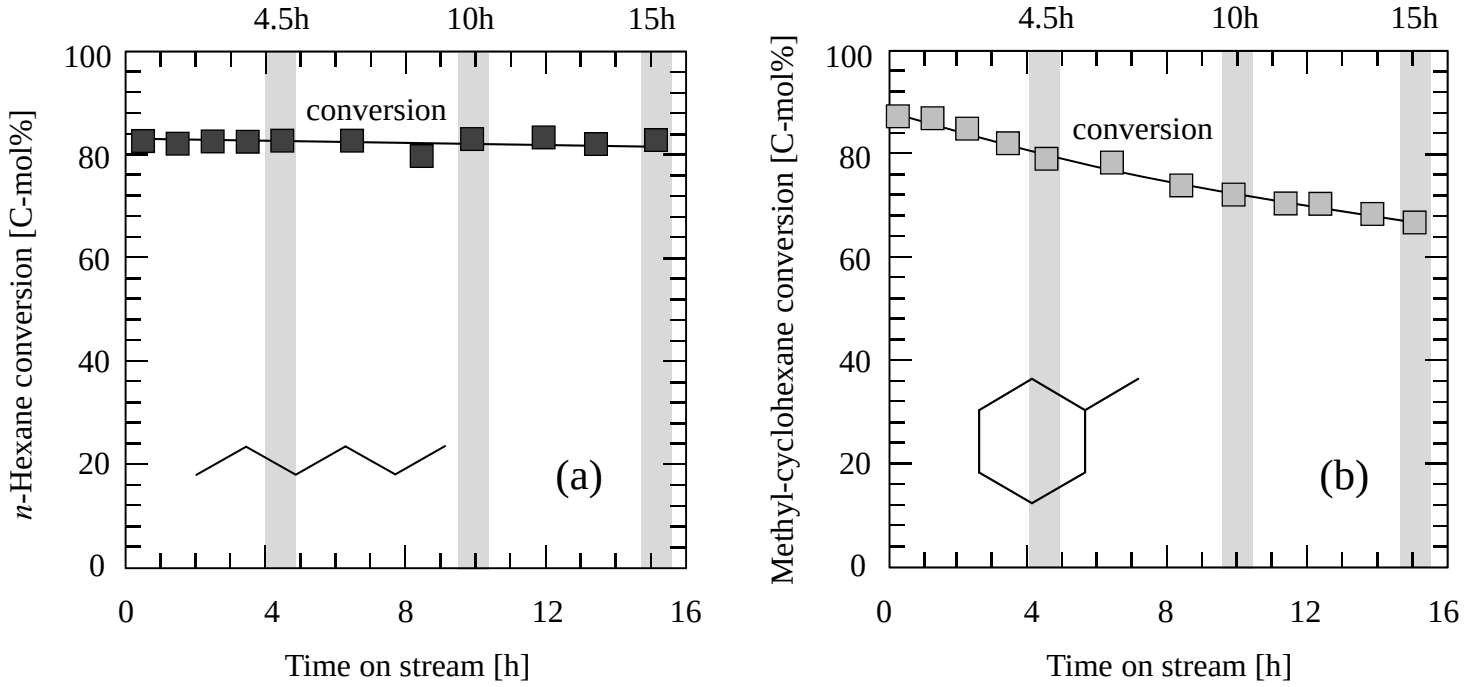

Fig. 8. (a) *n*-Hexane and (b) methyl-cyclohexane conversions with time on-stream (*W/F* = 0.125 h) over the nano-scale ZSM-5 zeolite (Si/Al = 150).

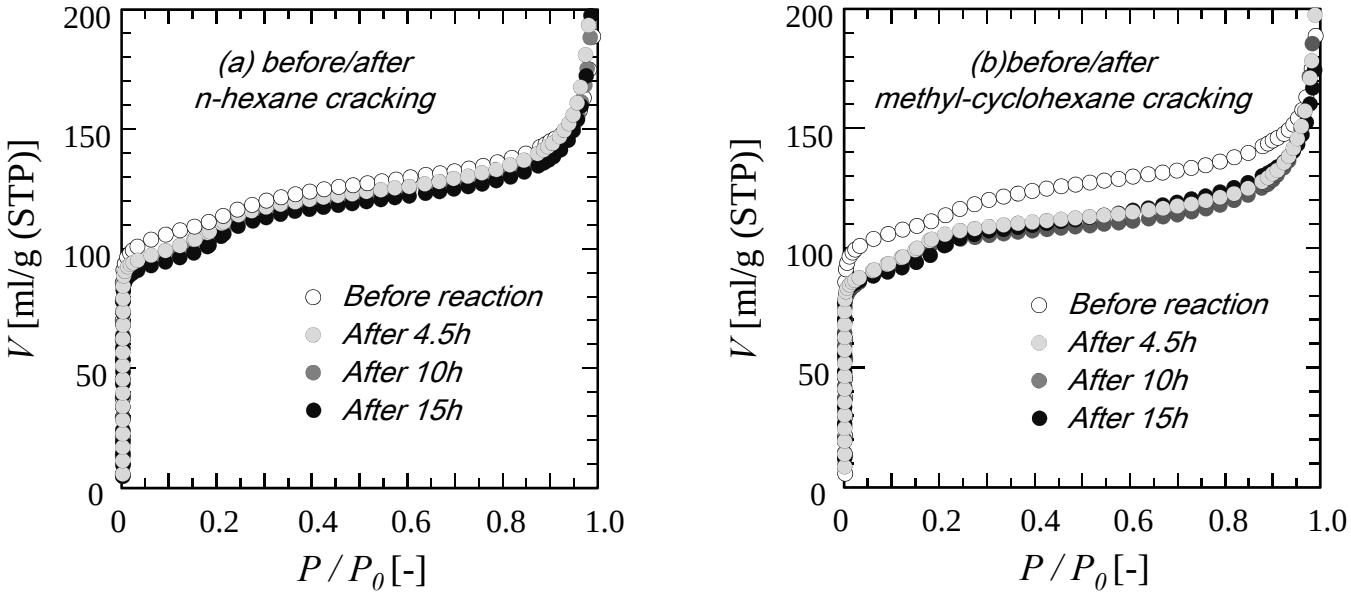

Fig. 9. N_2 adsorption isotherms of ZSM-5 zeolites before and after (a) *n*-hexane and (b) methyl-cyclohexane cracking reactions (4.5 h, 10 h, and 15 h).

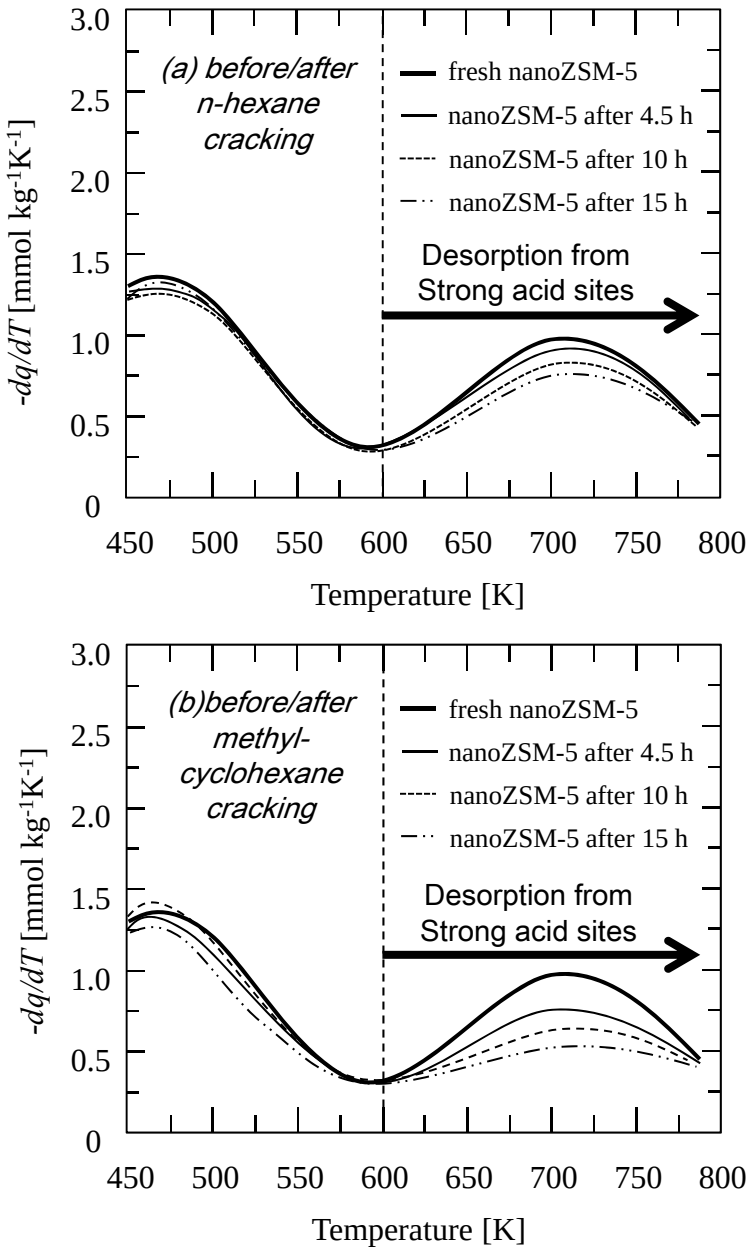

Fig. 10. NH_3-TPD profiles of nano-scale ZSM-5 zeolites (Si/Al = 150) before and after (a) *n*-hexane and (b) methyl-cyclohexane cracking reactions.